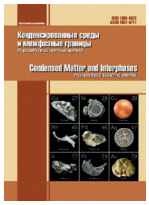

ISSN 1606-867X (Print)
ISSN 2687-0711 (Online)
Condensed Matter and Interphases
Kondensirovannye Sredy i Mezhfaznye Granitsy
https://journals.vsu.ru/kcmf/

Original articles

Research article
https://doi.org/10.17308/kcmf.2022.24/10555

Photosensitisation of reactive oxygen species with titanium dioxide nanoparticles decorated with silver sulphide quantum dots

O. V. Ovchinnikov, M. S. Smirnov, A. S. Perepelitsa✉, S. V. Aslanov✉, A. P. Gureev, V. N. Popov, F. A. Tsybenko, A. M. H. Hussein

Voronezh State University,
1 Universitetskaya pl., Voronezh, 394018, Russian Federation

Abstract

At present, the development of methods for sensitisation to the visible and IR spectral regions of systems for the photocatalytic production of reactive oxygen species based on titanium dioxide nanoparticles is of great interest. The purpose of this work was to establish the regularities of the photogeneration of reactive oxygen species during the formation of TiO_2 nanoparticle – Ag_2S quantum dots nanoheterosystems under the action of radiation in visible and near-infra-red spectral regions.

The paper analyses the photocatalytic properties of anatase nanoparticles 10–15 nm in size decorated with colloidal Ag_2S quantum dots with an average size of 2.5 nm passivated with thioglycolic and 2-mercaptopropionic acids. Selective sensor dyes were used to estimate the effectiveness of sensitisation of various reactive oxygen species with the studied photocatalysts under excitation in the UV and visible region. It was shown that decorating TiO_2 nanoparticles with quantum dots leads to an increased efficiency of the production by the system of hydroxyl radical, superoxide anion, and hydrogen peroxide under photoexcitation in the TiO_2 absorption region (UV range). Sensitisation of the production of reactive oxygen species by nanosystems was detected during excitation by radiation in the visible spectral region (outside the intrinsic TiO_2 absorption band). It was also found that there is an increase in the efficiency of the production of reactive oxygen species (up to 1.5 times) when thioglycolic acid is replaced with 2-mercaptopropionic acid as a passivator of Ag_2S quantum dots. The obtained data were used to develop a schematic diagram of photoprocesses in the system.

Keywords: Reactive oxygen species, Photocatalysis, Nanoparticles, Titanium dioxide, Quantum dots, Silver sulphide, Photosensitisation

Funding: This work was supported by the Russian Foundation for Basic Research grant No. 20-32-90167 “Postgraduate students”.

Acknowledgements: The studies of structural properties conducted by the methods of transmission electron microscopy and X-ray diffractometry were carried out using the equipment of the VSU Centre for Collective Use of Scientific Equipment.

For citation: Ovchinnikov O. V., Smirnov M. S., Perepelitsa A. S., Aslanov S. V., Gureev A. P., Popov V. N., Tsybenko F. A., Hussein A. M. H. Photosensitisation of reactive oxygen species with titanium dioxide nanoparticles decorated with silver sulphide quantum dots. *Condensed Matter and Interphases.* 2022;24(4): 511–522. https://doi.org/10.17308/kcmf.2022.24/10555

Для цитирования: Овчинников О. В., Смирнов М. С., Перепелица А. С., Асланов С. В., Гуреев А. П., Попов В. Н., Цыбенко Ф. А., Хуссейн А. М. Х. Фотосенсибилизация активных форм кислорода наночастицами диоксида титана, декорированными квантовыми точками сульфида серебра. *Конденсированные среды и межфазные границы*. 2022;24(4): 511–522. https://doi.org/10.17308/kcmf.2022.24/10555

✉ Alexei S. Perepelitsa, e-mail: a-perepelitsa@yandex.ru
✉ Sergei V. Aslanov, e-mail: windmaster7@yandex.ru

1. Introduction

Currently, scientists are actively developing hybrid nanosystems for photovoltaics and photocatalysis applications [1–4]. They are also studying the possibility of using them in clean-up systems [5–7], hydrogen production systems [8–10], for the creation of photobactericidal coatings and systems used to produce reactive oxygen species [11, 12]. Titanium dioxide (TiO_2) has been recognised as being the most suitable for such applications [13, 14]. However, the edge of photosensitivity for titanium dioxide (anatase and rutile) is about 3.1–3.2 eV [15, 16]. Therefore, there is a practically important problem of photosensitising TiO_2 to visible and IR radiation. Such photosensitisers can be organic dyes [1, 2, 4], plasmonic nanoparticles [17, 18], metal ions [19, 20], and semiconductor quantum dots (QDs) [23, 24].

Ag_2S QDs are appropriate for sensitising TiO_2 to the visible region. Silver sulphide is non-toxic, insoluble in water, chemically stable, and has the band gap of a massive crystal equal to 1.0 eV [25]. Ag_2S QDs have size-dependent luminescent and absorption properties [26] and can excite TiO_2 throughout the visible and near-infra-red region.

Silver sulphide is mainly considered for use as a sensitiser for heterosystems based on Ag_2S epitaxial nanoparticles which are grown or deposited on the surface of TiO_2 nanoparticles (NPs). As a rule, large Ag_2S nanoparticles are used, of about 5 nm in size and over that hardly have any size effect [27–33]. There are practically no publications devoted to the consideration of the photocatalytic properties of nanosystems based on TiO_2 nanoparticles (NPs) decorated with colloidal silver sulphide QDs 1–4 nm in size. In addition, the influence of QD passivators on the photocatalytic properties of the TiO_2 NP – Ag_2S QDs nanosystems still has not been established. Due to the significant nonstoichiometry, Ag_2S QDs are characterised by the presence of a large concentration of defects whose levels can participate in photocatalytic reactions [34] and manifest themselves in the recombination luminescence of the QDs [26, 35, 36]. Thus, it is important to obtain Ag_2S QDs with an interface structure that provides adsorption on the TiO_2 surface and effective photosensitisation of the production of reactive oxygen species.

The purpose of this work was to establish the patterns of photosensitisation of reactive oxygen species (ROS) during the formation of the TiO_2 NP – Ag_2S QDs nanoheterosystems when the latter are passivated with thioglycolic and 2-mercaptopropionic acids.

2. Experimental

2.1. Methods for sample synthesis

Used reagents: silver nitrate ($AgNO_3$), thioglycolic acid (TGA), 2-mercaptopropionic acid (2MPA), sodium sulphide (Na_2S), titanium tetrachloride ($TiCl_4$), absolute ethanol, ammonium hydroxide (NH_4OH), sodium hydroxide (NaOH), 5-amino-2,3-dihydro-1,4-phthalazinedione (luminol), 2H-1-benzopyranone-2 (coumarin), imidazole, 4-nitroso-N,N-dimethylaniline (RNO) were purchased from Sigma-Aldrich and were used without further purification. Amplex UltraRed and horseradish peroxidase were purchased from Thermofisher Scientific.

Colloidal Ag_2S QDs passivated with thioglycolic (hereinafter Ag_2S/TGA) and 2-mercaptopropionic (hereinafter Ag_2S/2MPA) acids were synthesised in water using Na_2S as a source of sulphur with the mixture pH of 10 [36]. During the last stage, 50 ml of 1 μM aqueous Na_2S solution was added to the reaction mixture to achieve QDs with an average size of about 2.5 nm. The QDs were then purified from the reaction products by centrifugation and subsequent dissolution in water.

TiO_2 NPs were synthesised using the sol-gel method by means of titanium tetrachloride hydrolysis. As part of a typical approach, 3.5 ml of $TiCl_4$ was dissolved in 35 ml of absolute ethanol in an ice bath at 0 °C. The gel was kept for 5 days in a refrigerator and dried at 80 °C. The collected white TiO_2 crystals were washed several times in distilled water and centrifuged to remove residual reaction products. They were then annealed in air for 2 hours at 400 °C to form a crystalline anatase structure and remove organic impurities. The collected fine crystalline powder was sonicated at 60 kHz for an hour to separate stuck nanoparticles.

To obtain the TiO_2–Ag_2S nanoheterosystems (hereinafter referred to as NSs), the TiO_2 NP powder was dissolved in water and sonicated for half an hour until a uniform suspension was obtained. After that, the solution of TiO_2 NPs

was mixed with the solution of QDs at the rate of 10 Ag_2S QDs per 1 TiO_2 NP and dried at the temperature of 65 °C with constant stirring. The resulting powder was ground in a mortar, sonicated for an hour, and washed with distilled water.

2.2. Equipment and experimental techniques

The OceanOptics USB2000+XR1 fiber spectrometer (Ocean Optics, USA) equipped with a USB-DT light source and an IS80 integrating sphere was used to measure optical absorption spectra and diffuse reflection spectra in the range of 200–900 nm. Barium sulphate powder (P.A.) was used as a white standard. The measured diffuse reflection spectra were rearranged as the $F(\hbar\omega)$ function known as the Kubelka–Munk function [37]:

$$F(R) = \frac{k}{s} = \frac{1-R^2}{2R},$$

where R is the diffuse reflection, k is the absorption coefficient, and s is the scattering coefficient. The position of the band gap was estimated by plotting the $\alpha^{1/2}(\hbar\omega) = F(\hbar\omega)\cdot\hbar\omega$ dependencies where $F(\hbar\omega)$ is the Kubelka–Munk function of the diffuse reflection spectrum. The linear part of the function was approximated by a straight line to the intersection with the x-axis [38].

A computer-aided spectrometric system based on a MDR-4 diffraction monochromator (Lomo, Russia) with a PDF10/C semiconductor low-noise photodiode (ThorLabs, USA) as a detector was used to measure luminescence spectra in the range of 700–1200 nm. A NDB7675 laser diode (Nichia, Japan) with the wavelength of 462 nm was used as a source of luminescence excitation. A Nichia NCSU276C LED module (Nichia, Japan) with the wavelength of 365 nm, TDS-P001L4G05 LED module (TDS Lighling Co., China) with the wavelength of 520 nm, and a LS-Xe-150 xenon lamp (OKB Spektr, Russia), equipped with interference filters were used to stimulate the production of reactive oxygen species of TiO_2 NPs.

Luminescence quantum yield was measured using a standard method of comparing with a reference [39]. A solution of indocyanine green in dimethyl sulfoxide with a luminescence quantum yield of 13% was used as a reference [40].

The production of superoxide anion ($O_2^{\bullet -}$) was measured by the chemiluminescent method using luminol [41]. The integral intensity of chemiluminescence was recorded using an R928P photoelectron multiplier (Hamamatsu, Japan) operating in photon counting mode.

Hydrogen peroxide (H_2O_2) was detected with an Amplex UltraRed selective sensor [42]. The luminescence intensity was recorded at the wavelength of 596 nm.

The concentration of hydroxyl radical (·OH) was determined by the luminescence of 7-hydroxycoumarin (7HC) in the 470 nm region [43].

The concentration of singlet oxygen ($^1O_2$) was measured by the absorption method using an imidazole solution with the addition of 4-nitroso-N,N-dimethylaniline (RNO) dye [44] in a ratio of 160:1. The measurement was made by decreasing the optical density of RNO absorption band in the 445 nm region.

The structural properties of the samples were examined by transmission electron microscopy (TEM) using a LIBRA 120 transmission electron microscope (CarlZeiss, Germany) and by X-ray diffractometry (XRD) using a THERMO ARL X'TRA X-ray diffractometer (Thermofisher Scientific, Switzerland).

3. Results and Discussion

3.1. Structural properties of the studied samples

The structure of the synthesised TiO_2 NPs was examined by X-ray diffraction. Figure 1 shows the X-ray diffraction pattern obtained for the K_{α_1} emission of copper (1.054 Å).

The analysis of diffraction patterns showed the presence of reflexes corresponding to the anatase crystal lattice broadened due to the small size of nanoparticles [45]. Size estimation by the Scherrer formula:

$$d = \frac{0.9\lambda}{\beta\cos\theta},$$

where β is the half-width of the reflection, λ is the wavelength of radiation (K_{α_1} Cu, 1.054 Å), θ is the diffraction angle, showed the presence of crystallites with an average size of about 12 nm. This is consistent with the TEM data for the images shown in Figure 2.

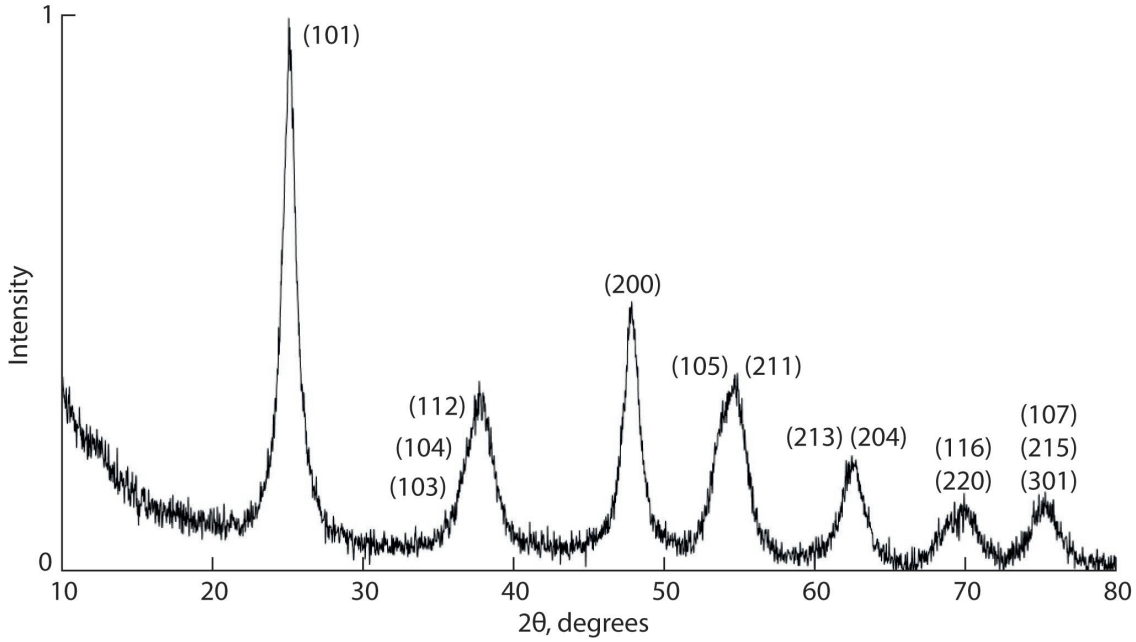

Fig. 1. X-ray diffraction pattern of TiO_2 NPs

The analysis of TEM images showed that the TiO_2 NPs had a shape close to spherical and had an average size of about 11 nm with a dispersion of ~27%.

The samples of Ag_2S QDs had an average size of 2.5 nm with a dispersion in size of 35 and 40% for Ag_2S/2MPA and Ag_2S/TGA, respectively. The study of high-resolution TEM images showed the presence of diffraction of the crystallographic plane (121) of the monoclinic crystal modification of Ag_2S (space group $P2_1/c$ with an interplanar distance of ~0.27 nm). In the TEM images of the TiO_2-Ag_2S/2MPA and TiO_2–Ag_2S/TGA NSs, there were QD clusters near the surface of the TiO_2

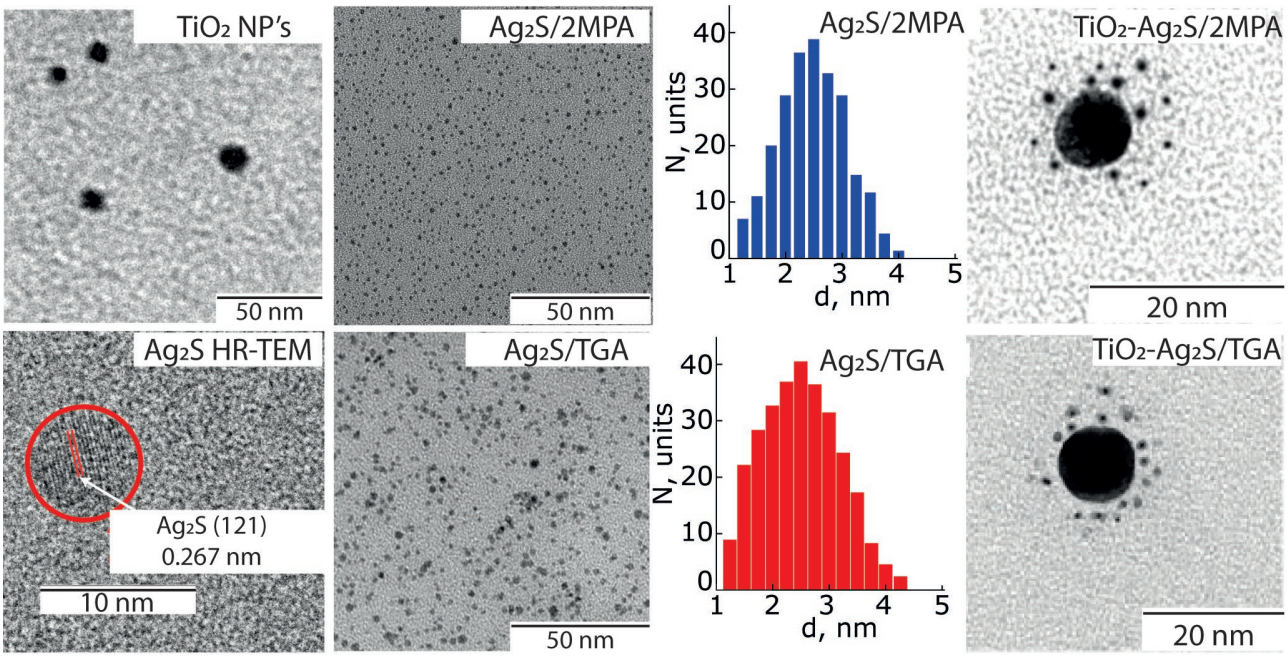

Fig. 2. TEM images of TiO_2 NPs, Ag_2S QDs, TiO_2–Ag_2S NSs, histograms of Ag_2S QD size distribution, and a high resolution TEM image of Ag_2S nanocrystal

nanoparticles. Thus, a conclusion can be made about the adsorption of Ag_2S QDs on the surface of the TiO_2 NPs.

3.2. Absorption and luminescence properties of the studied samples

Optical absorption spectra were broad bands with the absorption edge shifted towards the short-wave region relative to the absorption edge of massive Ag_2S (1.0 eV). In the 700 nm region (Fig. 3a), there were features associated with excitonic absorption. Using the data on the position of the exciton transition, the size of QDs was estimated using the effective mass approximation [46]:

$$E_g^{eff} = E_g^{bulk} + \frac{\hbar^2\pi^2}{2\mu R^2} + \frac{1.8e^2}{\varepsilon R} - 0.248E_{Ry}^*,$$

where E_g^{eff} is the peak exciton absorption, E_g^{bulk} is the width of the band gap of the bulk crystal, $\mu = \frac{m_{e^-}^* m_{h+}^*}{m_{e-}^* + m_{h+}^*}$. is the reduced effective mass of exciton, e is the charge of the electron, ε is the dielectric permeability, $E_{Ry}^* = \frac{e^4}{2\varepsilon^2\hbar^2(\frac{1}{m_{e-}^*} + \frac{1}{m_{h+}^*})}$ is Rydberg's effective energy. The average size for the Ag_2S/TGA QDs and Ag_2S/2MPA QDs was about 2.4 nm, which is close to the TEM data.

The edge of the absorption spectra obtained from diffuse reflection (Fig. 3b) for TiO_2 NPs was located in the region of 3.21 eV, which coincides with the data on the width of the band gap of anatase (3.2 eV) [14, 38]. The absorption spectra of TiO_2–Ag_2S/2MPA and TiO_2-Ag_2S/TGA NSs (Fig. 3b) had complex structure and were not a simple superposition of the absorption spectra of Ag_2S QDs and TiO_2 NPs. Such spectral behaviour can be a result of the formation of agglomerates of Ag_2S QDs during their adsorption on the surface of TiO_2 NPs. It can indicate the emergence of charge carrier transitions between the components of the TiO_2 NP– Ag_2S QDs hybrid system.

In the luminescence spectra of the Ag_2S/2MPA and Ag_2S/TGA QD samples (Figure 4), luminescence bands were observed with their maxima at 890 nm (1.39 eV) and 980 nm (1.27 eV) and quantum yields of 0.14 and 0.06%, respectively. The value of the Stokes shift of the luminescence peak (0.4–0.5 eV) and the half-width of the emission band of ~ 0.3 eV indicate the trap state nature of luminescence [26]. It is worth noting the fact that when the average size of QDs in the samples was the same, the luminescence peaks were shifted by 90 nm relative to each other, which indicates the influence of the surface environment on the energy of the luminescence centre [26, 35, 36, 47].

For Ag_2S/2MPA QDs, a 70-fold decrease in the luminescence quantum yield of Ag_2S QDs

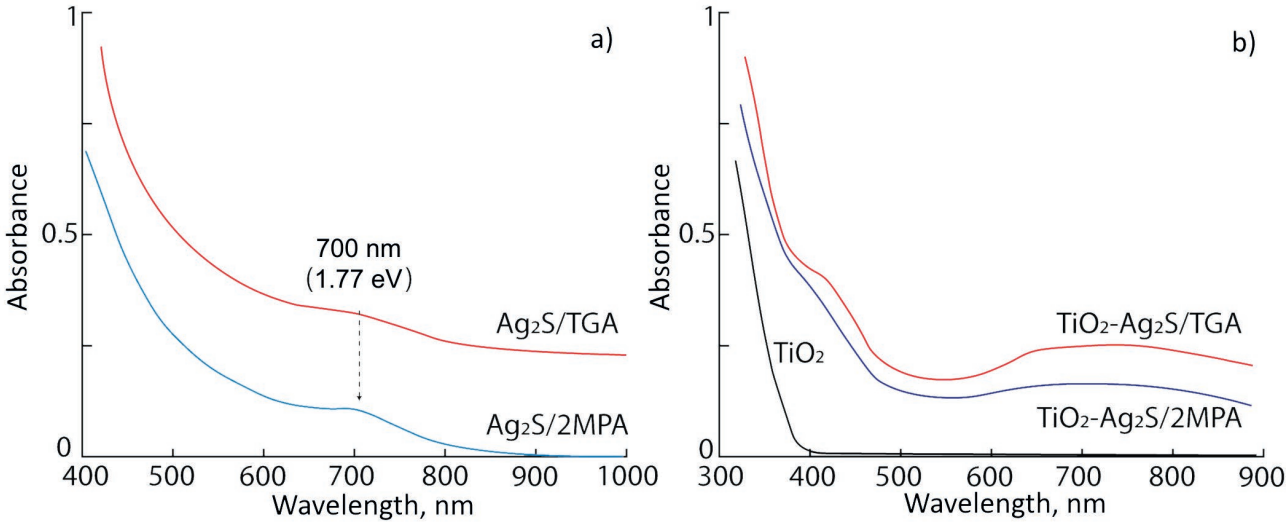

Fig. 3. (a) Optical absorption spectra of Ag_2S QDs. (b) Optical absorption spectra obtained using the method of diffuse reflection and the Kubelka–Munk equation for TiO_2 NPs, TiO_2–Ag_2S/2MPA NSs, and TiO_2–Ag_2S/TGA NSs

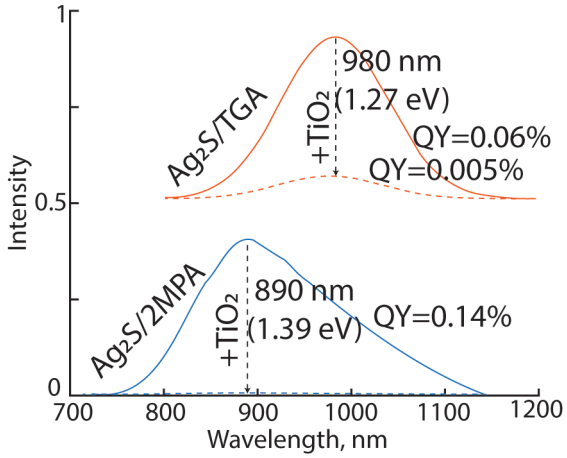

Fig. 4. Luminescence spectra of Ag_2S QDs and TiO_2–Ag_2S NSs

was observed when they were used to decorate TiO_2 NPs. For Ag_2S/TGA QDs, there was a 12-fold decrease. A significant luminescence quenching indicates the formation of charge transfer channels in the nanoheterosystem. Thus, during the formation of TiO_2–Ag_2S/2MPA and TiO_2-Ag_2S/TGA NSs, there was a transformation of the structure of the optical absorption spectra of the NS components and luminescence quenching of Ag_2S QDs.

3.3. ROS Sensitisation with the studied samples of the TiO_2–Ag_2S nanoheterosystems

Figure 5 shows the results of measurements of ROS generation by nanoheterosystems during excitation in the absorption region of TiO_2 NPs. TiO_2 NPs in water exposed to radiation with the wavelength of 365 nm produced superoxide anion ($O_2^{\bullet-}$), singlet oxygen ($^1O_2$), hydroxyl radical (·OH), and hydrogen peroxide (H_2O_2), which is consistent with the data [13]. In the colloidal solutions of Ag_2S/2MPA and Ag_2S/TGA QDs, only the production of hydrogen peroxide was recorded (Fig. 5d), which had not been previously recorded for Ag_2S QDs in the literature. The formation of nanosystems led to a change in the efficiency of production of all types of ROS. When TiO_2–Ag_2S/2MPA NSs and TiO_2-Ag_2S/TGA NSs were excited in the absorption region of titanium dioxide, the production of superoxide anion accelerated by 1.24 and 1.2 times, the production of hydroxyl radical accelerated by 156 and 115 times, and the production of hydrogen peroxide accelerated by 4.14 and 3.4 times, respectively, relative to TiO_2 NPs. At the same time, there was a decrease in the efficiency of production of singlet oxygen by 2.1 and 1.25 times, respectively, for TiO_2–Ag_2S/2MPA NSs and TiO_2-Ag_2S/TGA NSs as compared to TiO_2 NPs.

When Ag_2S QDs and TiO_2–Ag_2S NSs were illuminated with the wavelength of 520 nm, the radiation which is only absorbed by Ag_2S QDs, certain types of ROS were generated (Fig. 6). Both types of Ag_2S QDs only produced hydrogen peroxide with nearly the same efficiency. Non-decorated TiO_2 NPs did not produce ROS under photoexcitation with the wavelength of 520 nm.

The formation of TiO_2–Ag_2S/2MPA NSs and TiO_2-Ag_2S/TGA NSs led to an increase in hydrogen peroxide generation by 44 and 38.5 for visible radiation (520 nm) as compared to the original Ag_2S/2MPA QDs and Ag_2S/TGA QDs. In addition,

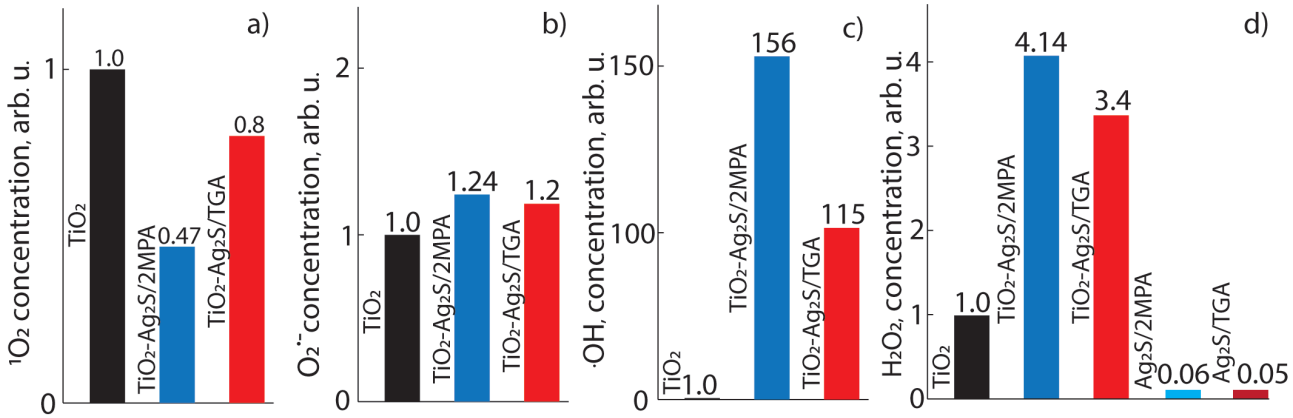

Fig. 5. Histograms of relative concentrations of ROS produced by Ag_2S QDs and TiO_2–Ag_2S NSs under excitation at λ = 365 nm: singlet oxygen (a), superoxide anion (b), hydroxyl radical (c), hydrogen peroxide (g). Histograms are normalised relative to TiO_2.

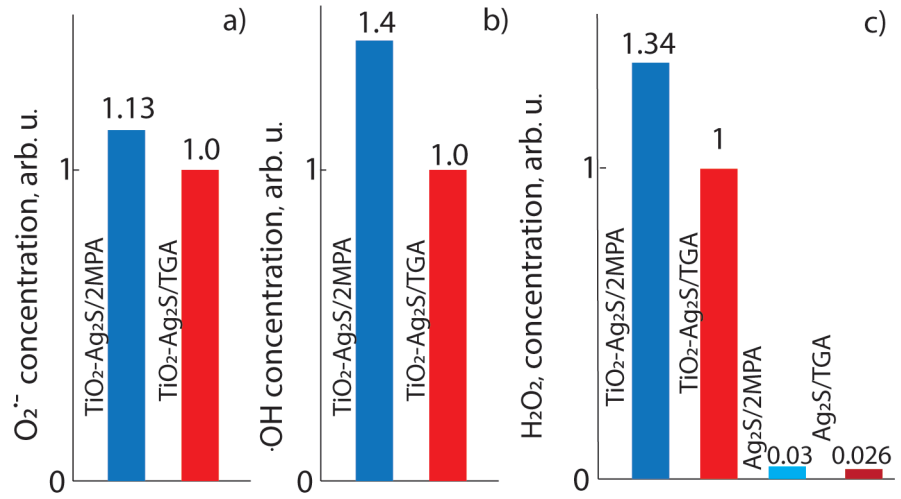

Fig. 6. Histograms of relative concentrations of ROS produced by Ag_2S QDs and TiO_2–Ag_2S NSs under excitation at λ = 520 nm: superoxide-anion (a), hydroxyl radical (b), hydrogen peroxide (c). Histograms are normalised relative to TiO_2-Ag_2S/TGA NSs

after decoration, anion superoxide and hydroxyl radical were formed, and the effectiveness of TiO_2–Ag_2S/2MPA NSs was respectively 1.13 and 1.4 times higher than of TiO_2–Ag_2S/TGA NSs. None of the samples produced singlet oxygen under the excitation with the wavelength of 520 nm.

3.4. ROS generation mechanisms in the studied nanoheterosystems

The analysis of data [48–54] allowed determining possible mechanisms of ROS production. Nanoheterosystems produce singlet oxygen only when excited in the UV region. What is more, the association with Ag_2S QDs results in reduced efficiency. This indicates a hole transfer from TiO_2 to Ag_2S and that the generation of $^1O_2$ in the system occurs due to the interaction of superoxide anion molecules with holes generated in TiO_2 under the action of excitation radiation, following the $O_2^{\bullet-} + h^+ \rightarrow {}^1O_2$ mechanism [53]. The absence of $^1O_2$ production when illuminated with visible radiation is determined by the absence of holes in TiO_2. To confirm this hypothesis, the generation of ROS in NSs was measured in the presence of a colloidal solution of a hole acceptor, 1% methanol (Fig. 7a). The introduction of 1% methanol resulted in a ninefold decrease in the efficiency of singlet oxygen generation for TiO_2, whereas for TiO_2–Ag_2S NSs there was a 20-fold decrease.

H_2O_2 production in Ag_2S/2MPA QDs and Ag_2S/TGA QDs was performed according to the

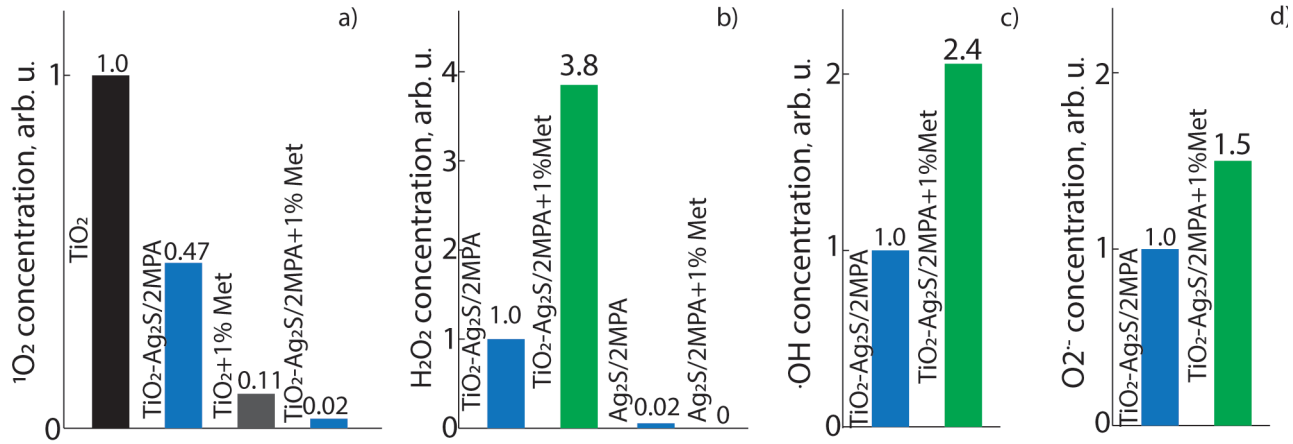

Fig. 7. ROS production by the samples of TiO_2 NPs and TiO_2-Ag_2S/2MPA NSs in the presence of a hole acceptor (methanol): singlet oxygen (λ_{exc} = 365 nm) (a), hydrogen peroxide (λ_{exc} = 520 nm) (b), hydroxyl radical (λ_{exc} = 520 nm) (c), anionic superoxide (λ_{exc} = 520 nm) (d)

reaction: $O_2 + 2H^+ + 2h^+ \rightarrow H_2O_2$ [53]. The fact that the reaction terminated when a hole acceptor was added speaks in favour of this theory (Fig. 7b). At the same time, it is likely that in NSs the process of H_2O_2 production took place on the surface of TiO_2 NPs during photoexcitation due to the reaction of $O_2^{\bullet-} + 2H^+ + e^- \rightarrow H_2O_2$ [53]. The 3.8-fold increase in the efficiency of production of H_2O_2 by TiO_2–Ag_2S NSs when a hole acceptor was added was probably due to the acceleration of hole recombination, and hence the increase in the number of electrons transferred to TiO_2.

The production of ·OH radicals occurred on the surface of TiO_2 by decomposition of hydrogen peroxide according to the reaction: $H_2O_2 + e^- \rightarrow {\cdot}OH + OH^-$ [53]. When 1% methanol was added, the production of ·OH radicals increased by 2.4 times, which was due to an increase in the concentration of peroxide in the solution.

Superoxide anion was generated by NSs on the surface of TiO_2 according to the reaction $O_2 + e^- \rightarrow O_2^{\bullet-}$ [53, 54] similar to the case of pure TiO_2 NPs. This is supported by the fact that $O_2^{\bullet-}$ was not generated by pure Ag_2S QDs. An increased production of $O_2^{\bullet-}$ under the action of UV radiation was due a more efficient electron transfer from Ag_2S QDs to TiO_2, NPs, which was indirectly confirmed by quenching QD luminescence during the assembly of NSs.

The proposed reactions were used to build a schematic diagram of photoprocesses in the TiO_2–Ag_2S NSs during excitation by radiation in the visible spectral region (Fig. 8). Photogenerated electrons pass from size quantization levels of Ag_2S QDs to the conduction band of TiO_2 NPs, where they localise in the near-surface layer and interact with the molecules of H_2O and O_2 dissolved in water, which is accompanied by the release of superoxide anion, hydroxyl radical, and hydrogen peroxide. The holes at the levels of size quantization of Ag_2S QDs interact with hydrogen ions and oxygen molecules, which results in the production of hydrogen peroxide. NSs are reduced due to the absorption from the environment (H_2O) of free charge carriers which are formed during the decomposition of short-lived ROS.

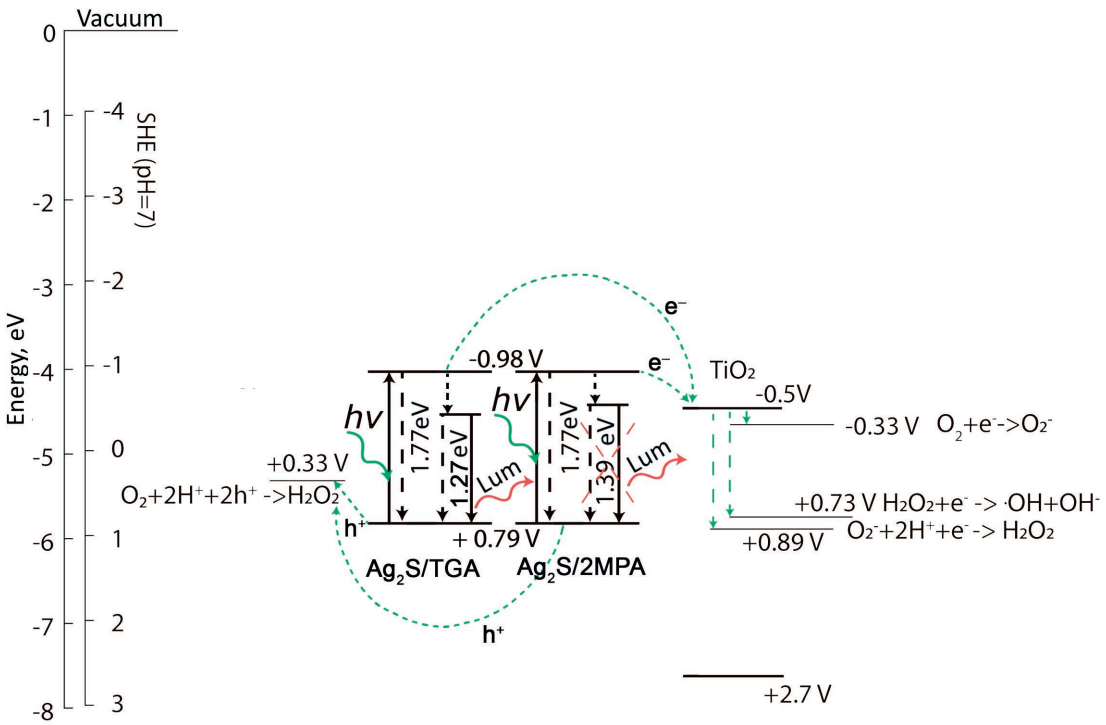

Fig. 8. Schematic diagram of photoprocesses and photocatalytic reactions in the studied samples of TiO_2–Ag_2S/2MPA NSs and TiO_2-Ag_2S/TGA NSs during excitation at λ = 520 nm. The data on redox potential and the location of bands were taken from [1, 2, 10, 25, 46, 48–54]

4. Conclusion

The study established new regularities of photosensitisation processes for reactive oxygen species of TiO_2 NPs (anatase) decorated with Ag_2S/2MPA and Ag_2S/TGA QDs. It was found that there is a decrease in the luminescence quantum yield of Ag_2S QDs (a 70-fold decrease for Ag_2S/2MPA QDs and a 12-fold decrease for Ag_2S/TGA QDs) when TiO_2 NPs are decorated, which indicates the separation of charge carriers between the nanosystem components. The photoexcitation of Ag_2S QDs is accompanied by the production of hydrogen peroxide. It was shown that the formation of TiO_2–Ag_2S NSs (when excited in the absorption region of TiO_2) leads to an increase in the efficiency of the production of superoxide anion by 1.2–1.4 times, hydrogen peroxide by 4–6 times, and hydroxyl radical by 100–150 times and reduces the efficiency of the production of singlet oxygen by up to two times. It was found that the excitation of the NSs in the visible region is accompanied by the photosensitisation of superoxide anions, hydroxyl radicals, and hydrogen peroxide, which does not happen in the case of TiO_2 NPs. It was noted that the type of surface environment of QDs affects the efficiency of the production of individual ROS: when the system is excited by radiation in the visible spectral region, NSs based on Ag_2S/2MPA QDs produce ROS 1.1–1.4 times more actively than NSs based on Ag_2S/TGA QDs. As a result of the study, we developed a schematic diagram of photoprocesses that determine ROS generation.

Author contributions

O. V. Ovchinnikov, head of scientific research, scientific editing of the text, discussion of the results of the study. M. S. Smirnov, scientific editing of the text, conducting experiments, discussion of the results of the study. S. V. Aslanov, conducting scientific research, writing the article. A. S. Perepelitsa, conducting scientific research, scientific editing of the text. A. P. Gureev, conducting experiments to measure the production of H_2O_2. V. N. Popov, discussion of the results, scientific editing of the text. F. A. Tsybenko, conducting scientific research. A. M. H. Hussein, conducting scientific research.

Conflicts of interest

The authors declare that they have no known competing financial interests or personal relationships that could have influenced the work reported in this paper.

References

1. *Nanomaterials for solar cell applications*. S. Thomas, E. H. M. Sakho, N. Kalarikkal, S. O. Oluwafemi, J. Wu (eds.). Amsterdam: Elsevier; 2019. https://doi.org/10.1016/C2016-0-03432-0

2. Yang D. *Titanium dioxide – material for a sustainable environment*. London: IntechOpen; 2018. 518 p. https://doi.org/10.5772/intechopen.70290

3. Roose B., Pathak S., Steiner U. Doping of TiO_2 for sensitized solar cells. *Chemical Society Reviews*. 2015;44: 8326–8349. https://doi.org/10.1039/C5CS00352K

4. Hou X., Aitola K., Lund P. D. TiO_2 nanotubes for dye-sensitized solar cells – A review. *Energy Science & Engineering*. 2021;9(7): 921–937. https://doi.org/10.1002/ese3.831

5. He F., Jeon W., Choi W. Photocatalytic air purification mimicking the self-cleaning process of the atmosphere. *Nature Communications*. 2021;12: 2528. https://doi.org/10.1038/s41467-021-22839-0

6. Ochiai T., Hoshi T., Silmen H., Nakata K., Murakami T., Tatejima H., Koide Y., Houas A., Horie T., Morito Y., Fujishima A. Fabrication of a TiO_2 nanoparticles impregnated titanium mesh filter and its application for environmental purification. *Catalysis Science & Technology*. 2011;1: 1324–1327. https://doi.org/10.1039/C1CY00185J

7. Stefanov B. *Photocatalytic TiO_2 thin films for air cleaning: Effect of facet orientation, chemical functionalization, and reaction conditions. Effect of facet orientation, chemical functionalization, and reaction conditions*. Doctor's thesis of philosoph. Digital Comprehensive Summaries of Uppsala Dissertations from the Faculty of Science and Technology. Uppsala: Acta Universitatis Upsaliensis; 1307. 2015. 148 pp.

8. Chiarello G. L., Dozzi M. V., Selli E. TiO_2-based materials for photocatalytic hydrogen production. *Journal of Energy Chemistry*. 2017;26(2): 250–258. https://doi.org/10.1016/j.jechem.2017.02.005

9. Kumaravel V., Mathew S., Bartlett J., Pillai S. C. Photocatalytic hydrogen production using metal doped TiO_2: A review of recent advances. *Applied Catalysis B: Environmental*. 2019;244(5): 1021–1064. https://doi.org/10.1016/j.apcatb.2018.11.080

10. Yu J., Qi L., Jaroniec M. Hydrogen production by photocatalytic water splitting over Pt/TiO_2 nanosheets with exposed (001) facets. *Journal of Phys-*

ical Chemistry C. 2010;114(30): 13118–13125. https://doi.org/10.1021/jp104488b

11. Binas V., Venieri D., Kotzias D., Kiriakidis G. Modified TiO_2 based photocatalysts for improved air and health quality. *Journal of Materiomics*. 2017;3(1): 3–16. https://doi.org/10.1016/j.jmat.2016.11.002

12. Magalhães P., Andrade L., Nunes O. C., Mendes A. Titanium dioxide photocatalysis: fundamentals and application on photoinactivation. *Reviews on Advanced Materials Science*. 2017;51(2): 91–129. Available at: https://ipme.ru/e-journals/RAMS/no_25117/01_25117_magalhaes.pdf

13. Nakata K., Fujishima A. TiO_2 photocatalysis: Design and applications. *Journal of Photochemistry and Photobiology C: Photochemistry Reviews*. 2012;13(3): 169–189. https://doi.org/10.1016/j.jphotochemrev.2012.06.001

14. Kapilashrami M., Zhang Y., Liu Y.-S., Hagfeldt A., Guo J. Probing the optical property and electronic structure of TiO_2 nanomaterials for renewable energy applications. *Chemical Review*. 2014;114: 9662–9707. https://doi.org/10.1021/cr5000893

15. Reddy K., Manorama S. V., Ramachandra Reddy A. Bandgap studies on anatase titanium dioxide nanoparticles. *Materials Chemistry and Physics*. 2003;78(1): 239–245. https://doi.org/10.1016/S0254-0584(02)00343-7

16. Zhu T., Gao S.-P. The stability, electronic structure, and optical property of TiO_2 Polymorphs. *Journal of Physical Chemistry C*. 2014;118(21): 11385–11396. https://doi.org/10.1021/jp412462m

17. Qin L., Wang G., Tan Y. Plasmonic Pt nanoparticles – TiO_2 hierarchical nano-architecture as a visible light photocatalyst for water splitting. *Scientific Reports*. 2018;8: 16198. https://doi.org/10.1038/s41598-018-33795-z

18. Yoo S. M., RawalaJ S. B., Lee J. E., Kim J., Ryu H.-Y., Park D.-W., Lee W. I. Size-dependence of plasmonic Au nanoparticles in photocatalytic behavior of Au/TiO_2 and Au@SiO_2/TiO_2. *Applied Catalysis A: General*. 2015;499: 47–54. https://doi.org/10.1016/j.apcata.2015.04.003

19. Khlyustova A., Sirotkin N., Kusova T. Doped TiO_2: the effect of doping elements on photocatalytic activity. *Materials Advances*. 2020;1: 1193–1201. https://doi.org/10.1039/D0MA00171F

20. Ansari S. A., Khan M. M., Ansari M. O., Cho M. H. Nitrogen-doped titanium dioxide (N-doped TiO_2) for visible light photocatalysis. *New Journal of Chemistry*. 2016;40: 3000–3009. https://doi.org/10.1039/C5NJ03478G

21. He J., Du Y., Bai Y., An J., Cai X., Chen Y., Wang P., Yang X., Feng Q. Facile formation of anatase/rutile TiO_2 nanocomposites with enhanced photocatalytic activity. *Molecules*. 2019;24: 2996. https://doi.org/10.3390/molecules24162996

22. Padayachee D., Mahomed A. S., Singh S., Friedrich H. B. Effect of the TiO_2 anatase/rutile ratio and interface for the oxidative activation of n-octane. *ACS Catalysis*. 2020;10(3): 2211–2220. https://doi.org/10.1021/acscatal.9b04004

23. Wageh S., Al-Ghamdi A. A., Soylu M., Al-Turki Y., Al-Senany N., Yakuphanoglu F. CdS quantum dots and dye co-sensitized nanorods TiO_2 solar. *Journal of Nanoelectronics and Optoelectronics*. 2014;9(5): 662–665. http://dx.doi.org/10.1166/jno.2014.1651

24. Zumeta-Dubé I., Ruiz-Ruiz V.-F., Díaz D., Rodil-Posadas S., Zeinert A. TiO_2 sensitization with Bi_2S_3 quantum dots: The inconvenience of sodium ions in the deposition procedure. *Journal of Physical Chemistry C*. 2014;118(22): 11495–11504. https://doi.org/10.1021/jp411516a

25. Guo Y., Lei H, Li B., Chen Z., Wen J., Yang G., Fang G. Improved performance in Ag_2S/P3HT hybrid solar cells with a solution processed SnO_2 electron transport layer. *RSC Advances*. 2016;6: 77701–77708. https://doi.org/10.1039/C6RA19590C

26. Ovchinnikov O. V., Smirnov M. S. IR luminescence mechanism in colloidal Ag_2S quantum dots. *Journal of Luminescence*. 2020;227: 117526. https://doi.org/10.1016/j.jlumin.2020.117526

27. Zhu L., Meng Z., Thisha G., Oh W.-C. Hydrothermal synthesis of porous Ag_2S sensitized TiO_2 catalysts and their photocatalytic activities in the visible light range. *Chinese Journal of Catalysis*. 2012;33(2–3): 254–260. https://doi.org/10.1016/S1872-2067(10)60296-3

28. Yadav S., Jeevanandam P. Synthesis of Ag_2S-TiO_2 Nanocomposites and their catalytic activity towards rhodamine B photodegradation. *Journal of Alloys and Compounds*. 2015;649: 483–490. https://doi.org/10.1016/j.jallcom.2015.07.184

29. Ghafoor S., Ata S., Manmood N., Arshad S. B. Photosensitization of TiO_2 nanofibers by Ag_2S with the synergistic effect of excess surface Ti^{3+} states for enhanced photocatalytic activity under simulated sunlight. *Scientific Reports*. 2017;7: 255. https://doi.org/10.1038/s41598-017-00366-7

30. Li Z., Xiong S., Wang G., Xie Z., Zhang Z. Role of Ag_2S coupling on enhancing the visible-light-induced catalytic property of TiO_2 nanorod arrays. *Scientific Reports*. 2016;6: 19754. https://doi.org/10.1038/srep19754

31. Dong M., Li Q.-H., Li R., Cui Y.-Q., Wang X.-X., Yu J.-Q., Long Y.-Z. Efficient under visible catalysts from electrospun flexible Ag_2S/TiO_2 composite fiber membrane. *Journal of Materials Science*. 2021;56: 7966–7981. https://doi.org/10.1007/s10853-021-05796-3

32. Zhu L., Meng Z.-D., Oh W.-C. MWCNT-Based Ag_2S-TiO_2 nanocomposites photocatalyst: ultrasound-assisted synthesis, characterization, and en-

hanced catalytic efficiency. *Journal of Nanomaterials*. 2012:586520. https://doi.org/10.1155/2012/586526

33. Yang M., Shi X. Biosynthesis of Ag_2S/TiO_2 nanotubes nanocomposites by Shewanella oneidensis MR-1 for the catalytic degradation of 4-nitrophenol. *Environmental Science and Pollution Research*. 2019;26(12): 12237–12246. https://doi.org/10.1007/s11356-019-04462-1

34. Tachan Z., Hod I., Shalom M., Grinis L., Zaban A. The importance of the TiO_2/quantum dots interface in the recombination processes of quantum dot sensitized solar cells. *Physical Chemistry Chemical Physics*. 2013;15(11): 3841. https://doi.org/10.1039/C3CP44719G

35. Ovchinnikov O. V., Aslanov S. V., Smirnov M. S., Grevtseva I. G., Perepelitsa A. S. Photostimulated control of luminescence quantum yield for colloidal Ag_2S/2-MPA quantum dots. *RSC Ad*vances. 2019;9: 37312–37320. https://doi.org/10.1039/C9RA07047H

36. Ovchinnikov O. V., Grevtseva I. G., Smirnov M. S., Kondratenko T. S., Perepelitsa A. S., Aslanov S. V., Khokhlov V. U., Tatyanina E. P., Matsukovich A. S. Effect of thioglycolic acid molecules on luminescence properties of Ag_2S quantum dots. *Optical and Quantum Electronics*. 2020;52: 198. https://doi.org/10.1007/s11082-020-02314-8

37. Kubelka P., Munk F. An article on optics of paint layers. *Fuer Tekn. Physik*. 1931;12: 593–609.

38. Murphy A. B. Band-gap determination from diffuse reflectance measurements of semiconductor films, and application to photoelectrochemical water-splitting. *Solar Energy Materials & Solar Cells*. 2007;91: 1326–1337. https://doi.org/10.1016/j.solmat.2007.05.005

39. Lakowitz R. *Principles of Fluorescent Spectroscopy* 3-ed. Springer; 2006. 954 pp.

40. Reindl S., Penzkofer A., Gong S.-H., Landthaler M., Szeimies R. M., Abels C., Bäumler W. Quantum yield of triplet formation for indocyanine green. *Journal of Photochemistry and Photobiology A: Chemistry*. 1997;105(1): 65–68. https://doi.org/10.1016/S1010-6030(96)04584-4

41. Bedouhene S., Moulti-Mati F., Hurtado-Nedelec M. , Dang P. M.-C., El-Benna J. Luminol-amplified chemiluminescence detects mainly superoxide anion produced by human neutrophils. *American Journal of Blood Research*. 2017;7(4): 41–48. Available at: https://www.ncbi.nlm.nih.gov/pmc/articles/PMC5545213/

42. Mohanty J. G., Jaffe J. S., Schulman E. S., Raible D. G. A highly sensitive fluorescent micro-assay of H_2O_2 release from activated human leukocytes using a dihydroxyphenoxazine derivative. *Journal of Immunological Methods*. 1997;202(2): 133–141. https://doi.org/10.1016/S0022-1759(96)00244-X

43. Wafi A., Szabó-Bárdos E., Horváth O., Makó E., Jakab M., Zsirka B. Coumarin-based quantification of hydroxyl radicals and other reactive species generated on excited nitrogen-doped TiO_2. *Journal of Photochemistry and Photobiology A: Chemistry*. 2021;404: 112913. https://doi.org/10.1016/j.jphotochem.2020.112913

44. Herman J., Neal S. L. Efficiency comparison of the imidazole plus RNO method for singlet oxygen detection in biorelevant solvents. *Analytical and Bioanalytical Chemistry*. 2019;411(20): 5287–5296. https://doi.org/10.1007/s00216-019-01910-2

45. Ijadpanah-Saravi H., Safari M., Khodadadi-Darban A., Rezaei A. Synthesis of titanium dioxide nanoparticles for photocatalytic degradation of cyanide in wastewater. *Analytical Letters*. 2014;47(10): 1772–1782. https://doi.org/10.1080/00032719.2014.880170

46. Kayanuma Y. Quantum-size effects of interacting electrons and holes in semiconductor microcrystals with spherical shape. *Physical Review B*. 1988;38(14): 9797–9805. https://doi.org/10.1103/PhysRevB.38.9797

47. Ovchinnikov O. V., Smirnov M. S., Aslanov S. V. Luminescence quantum yield and recombination constants in colloidal core/shell Ag_2S/ZnS and Ag_2S/SiO_2 quantum dots. *Optics and Spectroscopy*. 2020;128: 2028–2035. https://doi.org/10.1134/S0030400X2012098X

48. Athanasekou C. P., Likodimos V., Falaras P. Recent developments of TiO_2 photocatalysis involving advanced oxidation and reduction reactions in water. *Journal of Environmental Chemical Engineering*. 2018;6(6): 7386–7394. https://doi.org/10.1016/j.jece.2018.07.026

49. Turrens J. F. Mitochondrial formation of reactive oxygen species. *The Journal of Physiology*. 2003;552(2): 335-44. https://doi.org/10.1113/jphysiol.2003.049478

50. Fujishima A., Zhang X., Tryk D. A. TiO_2 photocatalysis and related surface phenomena. *Surface Science Reports*. 2008;63(12): 515–582. https://doi.org/10.1016/j.surfrep.2008.10.001

51. Kohtani S., Yoshioka E., Miyabe H. Photocatalytic hydrogenation on semiconductor particles. In: *Hydrogenation* (ed. I. Karame). *IntechOpen*. 2012. 340 pp. https://doi.org/10.5772/45732

52. Bard A. J., Parsons R., Jordan J. *Standart potentials in aqueous solutions*. Routledge, 1985. 848 pp. https://doi.org/10.1201/9780203738764

53. Nosaka Y., Nosaka A. Y. Generation and detection of reactive oxygen species in photocatalysis. *Chemical Reviews*. 2017;117: 11302–11336. https://doi.org/10.1021/acs.chemrev.7b00161

54. Belovolova L. V. Reactive oxygen species in aqueous media (A Review). *Optics and Spectroscopy*. 2020;128: 932–951. https://doi.org/10.1134/S0030400X20070036

Information about the authors

Oleg V. Ovchinnikov, Dr. Sci. (Phys.–Math.), Professor, Dean of the Faculty of Physics, Voronezh State University (Voronezh, Russian Federation).
https://orcid.org/0000-0001-6032-9295
ovchinnikov_o_v@rambler.ru

Mikhail S. Smirnov, Dr. Sci. (Phys.–Math.), Associate Professor, Associate Professor of the Department of Optics and Spectroscopy,, Voronezh State University (Voronezh, Russian Federation).
https://orcid.org/ 0000-0001-8765-0986
smirnov_m_s@mail.ru

Aleksey S. Perepelitsa, Cand. Sci. (Phys.–Math.), Senior Lecturer of the Department of Optics and Spectroscopy, Voronezh State University (Voronezh, Russian Federation).
https://orcid.org/ 0000-0002-1264-0107
a-perepelitsa@yandex.ru

Sergey V. Aslanov, graduate student of the Department of Optics and Spectroscopy, Voronezh State University (Voronezh, Russian Federation).
https://orcid.org/0000-0002-3961-2480
windmaster7@yandex.ru

Vasily N. Popov, Dr. Sci. (Biol.), Professor, Head of the Department of Genetics, Cytology and Bioengineering, Voronezh State University (Voronezh, Russian Federation).
https://orcid.org/0000-0003-1294-8686
pvn@bio.vsu.ru

Artem P. Gureev, Cand. Sci. (Biol.), Senior Lecturer of the Department of Genetics, Cytology and Bioengineering, Voronezh State University (Voronezh, Russian Federation).
https://orcid.org/0000-0003-3562-5329
gureev@bio.vsu.ru

Fedor A. Tsybenko, student of the Department of Optics and Spectroscopy, Voronezh State University (Voronezh, Russian Federation).
ozzy.642@yandex.ru

Alaa M. H. Hussein, graduate student of the Department of Optics and Spectroscopy, Voronezh State University (Voronezh, Russian Federation).
alaa.hussein@mail.ru

Received 24.06.2022; approved 20.07.2022; accepted 15.08.2022; published online 25.12.2022.

Translated by Irina Charychanskaya
Edited and proofread by Simon Cox